Chemistry & Biology
Brief Communication

How the Local Geometry of the Cu-Binding Site Determines the Thermal Stability of Blue Copper Proteins

Jesús Chaboy,[1,2,*] Sofía Díaz-Moreno,[3] I. Díaz-Moreno,[4] Miguel A. De la Rosa,[4] and Antonio Díaz-Quintana[4,*]
[1]Instituto de Ciencia de Materiales de Aragón, Consejo Superior de Investigaciones Científicas—Universidad de Zaragoza, 50009 Zaragoza, Spain
[2]Departmento Física de la Materia Condensada, Universidad de Zaragoza, 50009 Zaragoza, Spain
[3]Diamond Light Source Ltd., Harwell Science and Innovation Campus, Didcot, Oxfordshire OX11 0DE, UK
[4]Instituto de Bioquímica Vegetal y Fotosíntesis, Consejo Superior de Investigaciones Científicas—Universidad de Sevilla, 41092 Sevilla, Spain
*Correspondence: jchaboy@unizar.es (J.C.), qzaida@us.es (A.D.-Q.)
DOI 10.1016/j.chembiol.2010.12.006

SUMMARY

Identifying the factors that govern the thermal resistance of cupredoxins is essential for understanding their folding and stability, and for improving our ability to design highly stable enzymes with potential biotechnological applications. Here, we show that the thermal unfolding of plastocyanins from two cyanobacteria—the mesophilic *Synechocystis* and the thermophilic *Phormidium*—is closely related to the short-range structure around the copper center. Cu K-edge X-ray absorption spectroscopy shows that the bond length between Cu and the S atom from the cysteine ligand is a key structural factor that correlates with the thermal stability of the cupredoxins in both oxidized and reduced states. These findings were confirmed by an additional study of a site-directed mutant of *Phormidium* plastocyanin showing a reverse effect of the redox state on the thermal stability of the protein.

INTRODUCTION

In recent years our knowledge of the thermal stability of proteins has improved considerably. However, rational design of thermostable proteins remains elusive. Thermophilic organisms thrive at temperatures at which proteins from mesophilic organisms are often completely unfolded and nonfunctional. Understanding the mechanisms by which proteins develop thermal stability will help to optimize and design thermostable functional proteins for a variety of biotechnological applications (Adams and Kelly, 1995; Persidis, 1998; Szilagyi and Zavodszky, 2000; Lehmann et al., 2000; Tsujimura et al., 2008; Miura et al., 2009). For this purpose we need to clarify what factors make proteins from thermophilic organisms (thermophilic proteins) different from their mesophilic homologs. Previous work has shown that the overall structure of the native conformation is not a dominant factor because homologous proteins invariably adopt the same fold (Szilagyi and Zavodszky, 2000).

Blue Copper Proteins (BCPs) are of outstanding industrial interest, as putative components of biological fuel cells (Tsujimura et al., 2008; Miura et al., 2009). In fact the multicopper oxidases used for this purpose comprise functional BCP domains (Nakamura and Go, 2005; Kosman, 2010). Despite its role being barely understood, the copper site plays an essential part in the thermal stability of BCPs and in the kinetics of their unfolding process (Leckner et al., 1997; Pozdnyakova and Wittung-Stafshede, 2001; Pozdnyakova et al., 2001; Alcaraz and Donaire, 2004, 2005). Oxidized species of plastocyanin (Pc) from thermophilic cyanobacteria (Feio et al., 2004) are more thermally stable than their reduced forms, whereas the contrary occurs in Pc from plants (Sandberg et al., 2003) or mesophilic cyanobacteria (Feio et al., 2006). These different behaviors are unexpected because amino acids at the surroundings of the metal center are highly conserved in all these proteins (Figures 1A–1C).

Pcs contain a mononuclear copper site (type I) (Gough and Chotia, 2004) wherein the first coordination sphere of the metal ion is formed by two nitrogen atoms and two sulfur atoms in a distorted trigonal pyramid (Solomon et al., 2004; Solomon, 2006). In the reduced species, ligands to metal (dative) interactions involve 2p and 3p atomic orbitals (AOs) from ligands and the 4p AO from copper. Minor, if any, back-bonding from metal has been estimated (Guckert et al., 1995). In oxidized BCPs the anisotropy of the highest occupied molecular orbital (HOMO) of Cu^{2+} determines the physical and chemical properties of the metal center (Randall et al., 2000; Solomon et al., 2004; Solomon, 2006). This orbital lies over the equatorial plane containing the two nitrogen atoms and $S_{\gamma\text{-Cys}}$. Among the metal-ligand bonds, that involving $S_{\gamma\text{-Cys}}$ shows the largest degree of covalence, resulting from the combination of the copper $d_{x^2-y^2}$ AO with the $3p_{\pi}$ AO of $S_{\gamma\text{-Cys}}$ (Solomon et al., 2006; Pavelka and Burda, 2008). Opposite, the long axial Cu–$S_{\delta\text{-Met}}$ bond shows little covalent character. Although the Cu-$S_{\gamma\text{-Cys}}$ bond provides a high electronic coupling for electron transfer, the physiological electron exchange port locates in the histidine imidazol ligand that is partially exposed to solvent (Canters et al., 2000).

Theory also shows that the copper site geometry is somehow modulated by the overall protein scaffold (Comba, 2000). Studies on model systems show that there is a reciprocal relationship between Cu–$S_{\gamma\text{-Cys}}$ and Cu–$S_{\delta\text{-Met}}$ bond strengths. Distortion of the geometry alters the overlap between copper and ligand orbitals: the Cu $d_{x^2-y^2}$ AO tilts, and the Cu–$S_{\gamma\text{-Cys}}$ bond weakens, whereas that between Cu and $S_{\delta\text{-Met}}$

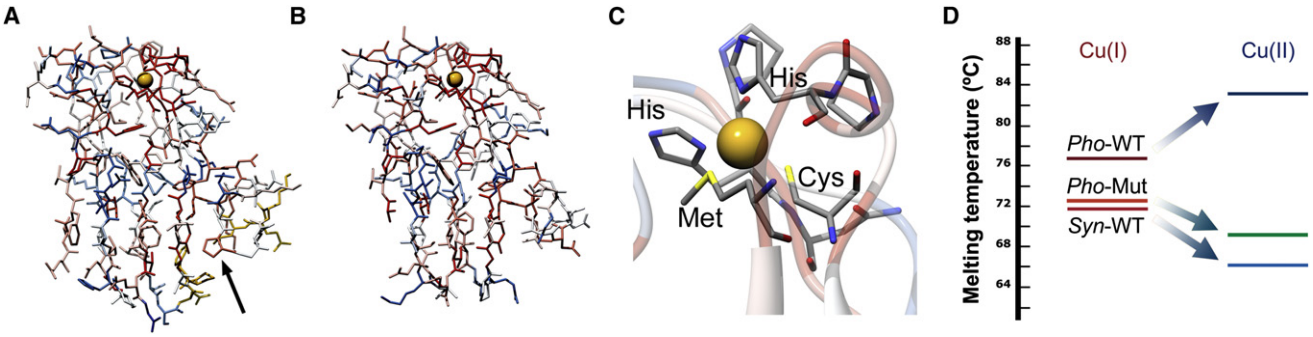

Figure 1. Comparison between Pcs from *Phormidium* and from *Synechocystis*

(A and B) Diagrams of (A) *Pho*-WT (pdb code: 1baw) and (B) *Syn*-WT (1pcs) Pcs (21, 22). Residues are colored according to conservation patterns from ConSurf phylogenetic computations, which include all the BCP family. Average residues are in white. Color scale corresponds to residues with increasing variability as compared to average. Red corresponds to highly conserved residues and blue to variable amino acids. ConSurf (Landau et al., 2005) calculations are unreliable for residues colored in yellow. Graphics are performed with UCSF Chimera (Pettersen et al., 2004). The arrow in (A) points to the location of the site-directed mutation.

(C) Detailed view of the copper site. Residues within 5 Å from the metal ion are represented in sticks. Those containing first-sphere atoms are labeled. Backbone ribbon is colored as in (A) and (B).

(D) Comparison of T_m values among Pc species (Feio et al., 2004, 2006; Muñoz-López et al., 2010a).

strengthens, or vice versa (LaCroix et al., 1996). Moreover, mutations of charged residues at the protein surface affect the Cu–$S_{\delta\text{-Met}}$ bond length while modulating the stability of BCPs (Sato and Dennison, 2002). Namely, a conserved lysine residue is essential for the correct folding of plant phytocyanins, which display glutamine instead of methionine as the axial ligand (Harrison et al., 2005). Of outstanding biotechnological interest is that the copper site environment can be modified to tune its acid-base properties and redox potential (Remenyi et al., 2001; Marshall et al., 2009), to lodge a different kind of copper center (Jones et al., 2003), or to improve the electron transfer rate of these proteins (Lancaster et al., 2009).

We have investigated by X-ray absorption spectroscopy (XAS) the relationship between the local geometry of the Cu site and the thermal unfolding behavior of the well-known copper-containing protein Pc from thermophilic (*Phormidium laminosum*, *Pho*-WT) and mesophilic (*Synechocystis* sp. PCC 6803, *Syn*-WT) cyanobacteria. We have previously shown that the higher thermal stability of *Pho*-WT is not related to typical structural adaptation patterns (Muñoz-López et al., 2010b). This study has also been extended to the double mutant P49G/G50P of *Phormidium* Pc (*Pho*-Mut) (Muñoz-López et al., 2010a). This mutation reverses the relationship between the oxidation state of copper and the thermal stability of the protein (Figure 1D). Because it lies far from the metal site (Figure 1A), it illustrates how the protein matrix affects the metal site. Our results show that the thermal stability of Pc is closely related to the bond length between Cu and the S atom from the cysteine acting as a ligand. Notably, the replacement of this residue is essential to enhance the capability of the protein for direct electron transfer to electrodes (Lancaster et al., 2009).

RESULTS AND DISCUSSION

Pho-WT shows a larger thermal stability than *Syn*-WT (Feio et al., 2004, 2006). The midpoint unfolding temperatures (T_m) represented in Figure 1D (see Table 1 for numerical values) show that reduced *Syn*-WT is more stable than its oxidized species. Opposite, in *Pho*-WT the oxidized form is the most stable one. Notably, T_m values of the *Pho*-Mut are, in both reduced and oxidized forms, closer to the T_m values of *Syn*-WT than to those of *Pho*-WT (Muñoz-López et al., 2010a). Interestingly, the largest T_m differences are found among the oxidized forms in all cases. In fact, reduced Pcs exhibit similar T_m values lying in between the two extreme corresponding to the oxidized forms.

Overall, Cu K-edge X-ray absorption near edge spectroscopy (XANES) spectra of the oxidized forms of *Pho*-WT, *Syn*-WT, and *Pho*-Mut Pcs (Muñoz-López et al., 2010a) are quite similar but show well-defined differences (Figure 2, upper panel). Indeed, the XANES spectrum of *Pho*-Mut perfectly overlaps with that of *Synechocystis* through all the spectral range. However, the spectrum of *Pho*-WT differs in the shape, intensity, and energy position of the shoulder-like feature (A) at the absorption threshold, the peak B, at ~9.5 eV above the edge, and of the main absorption line C (~18.5 eV) (see Figure 2). Actually, the B peak is clearly observed in both *Syn*-WT and *Pho*-Mut, but it is missing in the case of *Pho*-WT. The spectral shape and the intensities of the main absorption features in the near-edge region of the XAS spectra are extremely sensitive to changes of the local structure (Chaboy, 2009). Therefore, these results

Table 1. Melting Points (°C) of BCPs in This Work

Protein	Oxidized (Cu^{II}) Species	Reduced (Cu^{I}) Species
Pho-WT[a]	81.8 ± 0.4	75.7 ± 1.0
Pho-Mut[a]	69.1 ± 1.0	72.3 ± 1.1
Syn-Pc[b]	65.0 ± 1.0	71.3 ± 1.0

Values obtained by UV fluorimetry under the same buffer conditions used in the X-ray absorption experiments.

[a] Muñoz-López et al. (2010b); Feio et al. (2004).

[b] Feio et al. (2006). See Figure 1D for a graphic representation.

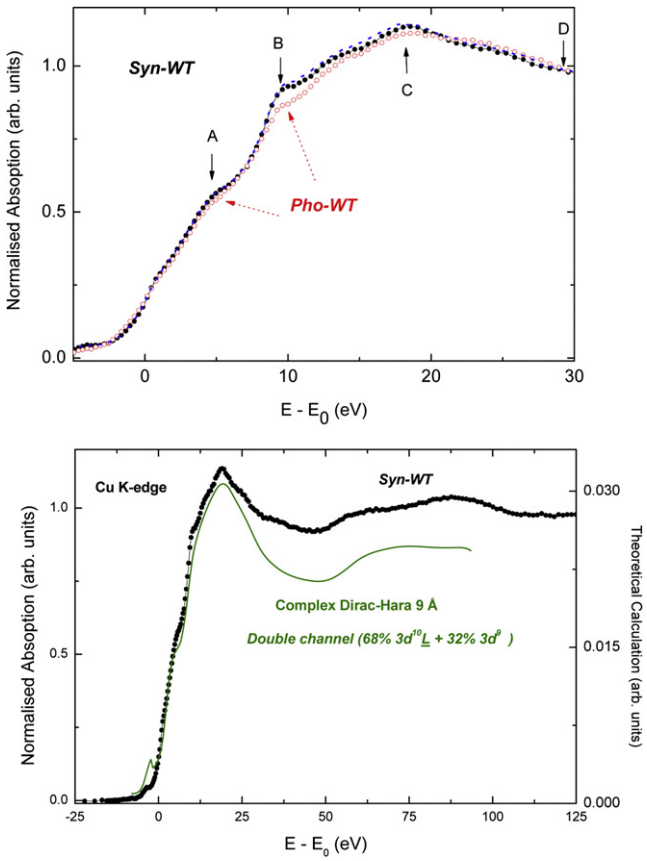

Figure 2. XANES Experiments

The top panel shows a detailed comparison of the experimental XANES spectrum at the Cu K-edge of Pc in *Syn*-WT (●) and *Pho*-WT (○). The dotted blue line corresponds to the spectrum recorded in the case of *Pho*-Mut. In all the cases the zero energy has been taken as E_0 = 8981eV. The bottom panel shows a comparison of the experimental XANES spectrum at the Cu K-edge in *Syn-WT* Pc (●) and the theoretical spectra (green, solid line) calculated by using a complex Dirac-Hara ECP potential within the two-channel approach (Chaboy et al., 2005, 2006a, 2006b). See also Figures S1 and S2.

indicate that the local structural environment of Cu is similar in both *Syn*-WT and *Pho*-Mut, as the thermal unfolding behavior is too, being unlike the one of *Pho*-WT. Moreover, despite the mutation of *Phormidium* taking place at distances greater than 20 Å away from the copper site, it induces a structural modification that is sensed by the metal ion. In this way the local structure around Cu in *Pho*-Mut is similar to that of *Syn*-WT and is different from that found in the unmodified *Pho*-WT's one. It should be noted that the mutation locates at a loop (L_5) settled at the end of the β strand that links it to a His residue acting as a copper ligand. However, the mutation does not affect the secondary structure substantially (Muñoz-López et al., 2010a). Noteworthy, molecular dynamics reports show concerted motions between loop L_5 and loops surrounding the copper site (Arcangeli et al., 2001), which are in agreement with the observed modification of the Cu environment obtained by XAS.

Bearing in mind the similarity of the T_m values of the oxidized forms of both *Syn*-WT and *Pho*-Mut, all these results suggest that the local environment details of Cu are linked to the thermal unfolding properties. Hence, we have performed ab initio computations of the Cu K-edge XANES spectra of these oxidized species to determine the origin of the differences observed in the XANES spectra, and to identify which individual structural component (histidines, cysteine, methionine) of the Cu environment is affected by the mutation of *Phormidium* that brings its behavior into a comparative agreement with *Synechocystis*. As shown in Figure 2, we have obtained an accurate reproduction of the experimental spectra of both *Syn*-WT and *Pho*-WT. As pointed out in Supplemental Experimental Procedures (available online), best agreement with the experimental spectra is obtained by using complex exchange and correlation (ECP) potentials in which the imaginary part accounts for the photoelectron damping (Figure S1). In addition it is necessary to include two different electronic configurations (3d10*L* and 3d9, where *L* denotes a 2p-hole in ligands) in order to get a correct description of the final state during the photo-absorption process (Figure S2). Hence, our next step was to determine how the Cu environment found in *Pho*-WT has to be modified in order to reproduce the experimental XANES spectra of its mutant form and of *Syn*-WT.

The Cu-binding site in BCPs features a distorted trigonal pyramid. Two nitrogen atoms ($N_{\delta1,HisN}$ and $N_{\delta2,HisC}$) from separate His residues and a sulfur atom ($S_{\gamma,Cys}$) from a Cys ligand represent the trigonal plane of the pyramidal base. A second sulfur ($S_{\delta,Met}$) atom from an axial Met residue forms the apex. Distortion occurs in the contact lengths between the copper and sulfur ligands being the Cu-$S_{\gamma,Cys}$ bond shorter than the Cu-$S_{\delta,Met}$ one. According to X-ray diffraction studies (Romero et al., 1998; Bond et al., 1999), the Cu-$S_{\sigma,Cys}$ interatomic distance is 2.10 Å in oxidized *Pho*-WT (Bond et al., 1999) (PDB code 1baw), shorter than that in oxidized *Syn*-WT (Romero et al., 1998) (PDB code 1pcs), which is 2.25 Å long. Conversely, the Cu-S_{Met} bond length in *Pho*-WT, 2.73 Å, is longer than in *Syn*-WT, 2.65 Å. Then, we have computed the Cu K-edge XANES of *Pho*-WT but replacing different coordination shells by those found in *Syn*-WT. In this way we have constructed three modified *Pho*-WT clusters containing 151 atoms, in which the first five, 14, and 112 next neighbors of Cu have been substituted by those found in *Synechocystis*. The results of these calculations are reported in Figure 3. Replacing the first 14 neighbors of Cu (atoms within 4 Å from the metal) allows us to reproduce the experimental spectra of *Syn*-WT. Exchanging further *Synechocystis*-like shells up to 8 Å has no significant effect on the calculated spectra. Next, we have calculated the Cu K-edge of a *Pho*-WT cluster in which we have specifically substituted the neighbors within the first 4 Å around the Cu ion coming from the His, Cys, and Met ligands. As shown in Figure 3 (middle panel), the substitution of Met coordinates has no effect on the spectrum. However, the modification of His or Cys neighbors changes the original *Pho*-WT spectrum to the one of *Syn*-WT. Specifically, after modifying the Cys ligand, the spectrum perfectly fits to the *Syn*-WT's one at the high-energy region. Finally, we have performed four similar computations in which only one atom is changed at each time: the $N_{\delta1}$ atoms associated to the two His and the S_γ and S_δ of Cys and Met, respectively. The results of these computations show that the modification of the Cu-$S_{\gamma,Cys}$ bond accounts for the differences found between *Syn*-WT and *Pho*-WT.

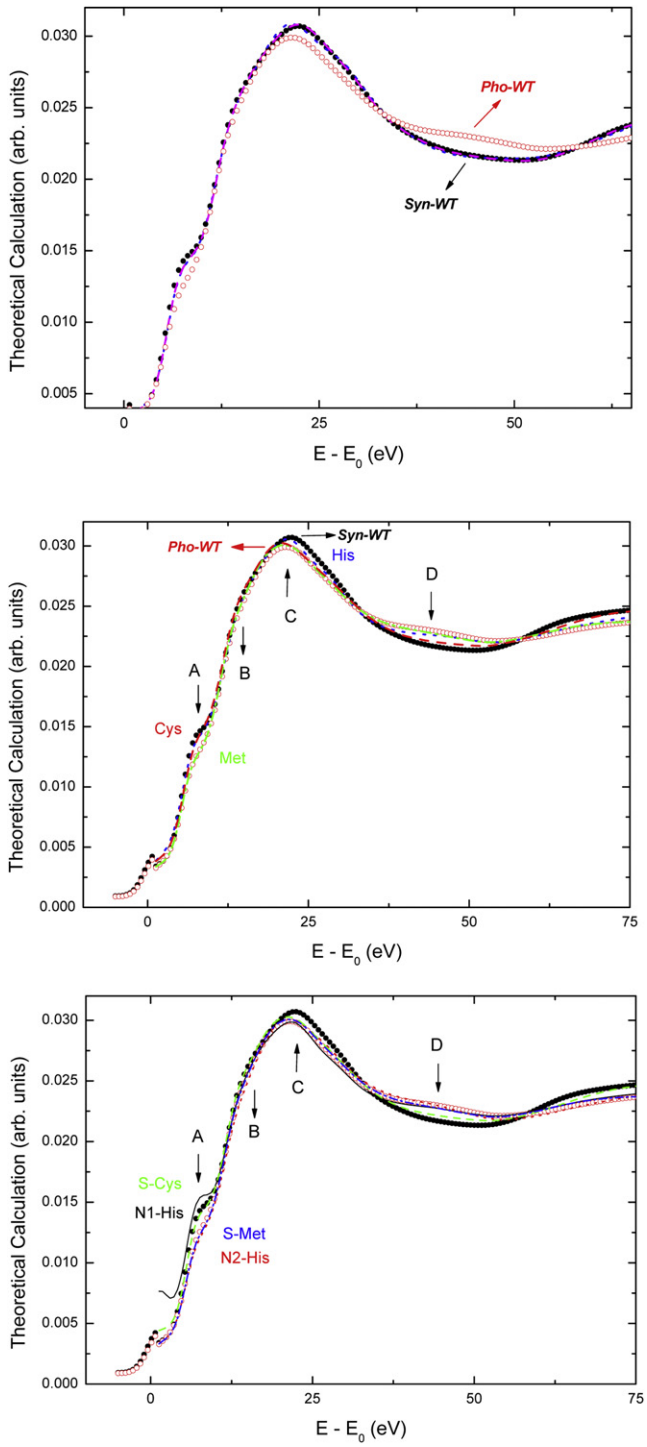

Figure 3. XANES of the Oxidized Forms

Comparison of the theoretical spectra calculated for Cu in *Syn*-WT (●) and *Pho*-WT (○) and those of: a 151 atom *Pho*-WT cluster in which the first 15 (blue, dots) and 113 (purple, dash) atoms have been substituted by the structural arrangement of *Syn*-WT (top panel); a 151 atom *Pho*-WT cluster in which the next neighbors associated to the histidines (blue, dots), cysteine (red, dash), and methionine (green, dot-dash) within the first 4 Å around the absorbing Cu have been substituted for those found in *Syn*-WT (middle panel); and of a 151 atom *Pho*-WT cluster in which the N atoms associated to the histidines (black, solid line, and red, dots), and the sulfur ones associated to cysteine (green, dash) and methionine (blue, dot-dash) have been substituted for those found in *Syn*-WT (bottom panel).

The picture emerging from the XANES results for the oxidized forms remarks that the length of the Cu-$S_{\gamma,Cys}$ bond is the essential parameter in determining the thermal stability of these BCPs. If this is the case, the Cu-$S_{\gamma,Cys}$ should also play a fundamental role into determining the thermal properties of the reduced forms. As shown in Figure 1C, the T_m values of the three reduced species are similar, and their values are between those of the oxidized forms of *Pho*-WT and *Syn*-WT or *Pho*-Mut. The above hypothesis entails that the lower T_m, the longer Cu-$S_{\gamma,Cys}$ bond length. In fact, oxidized *Syn*-WT shows the lowest T_m and the longest Cu-$S_{\gamma,Cys}$ (2.25 Å) bond length, whereas the highest T_m value and the shortest Cu-$S_{\gamma,Cys}$ bond (2.10 Å) correspond to oxidized *Pho*-WT. Then, it would be expected that the Cu-$S_{\gamma,Cys}$ bond length be similar in the three reduced forms and, in addition, intermediate between the two extremes of the oxidized species. The similarity of the Cu K-edge XANES of the reduced forms of *Pho*-WT, *Syn*-WT, and *Pho*-Mut, reported in Figure 4, supports this hypothesis because differences found in the near-edge region are less marked than for the oxidized forms. This is further supported by computations assuming identical Cu-$S_{\gamma,Cys}$ bond lengths in the three proteins. Starting from the Cu environment of oxidized *Pho*-WT and *Syn*-WT, changes of the Cu-$S_{\delta,Met}$ bond length do not affect the spectral profile. However, when the Cu-$S_{\gamma,Cys}$ length is fixed to an intermediate value (2.17 Å) the spectra of both *Pho*-WT and *Syn*-WT perfectly match at the threshold region in which the major differences in the Cu K-edge absorption of the oxidized form were observed.

In summary, our results provide evidence of the relationship between the thermal unfolding behavior and the different local geometry of the Cu-binding site in mesophilic and thermophilic proteins. This finding shows how the interplay between the metal center and the polypeptide chain determines the thermal stability of the holoprotein and how it is affected by the oxidation state of the metal atom, suggesting a means to perform rational design of type I copper enzymes of industrial interest.

SIGNIFICANCE

The development of biological fuel cells is an area of intensive current research, and multicopper oxidases are a promising key component of such devices (Tsujimura et al., 2008; Miura et al., 2009). The type I copper site is the active catalytic center that oxidizes substrates in these enzymes, which also have the ability to reduce molecular oxygen to water (Kosman, 2010) and to transfer electrons directly to the electrodes of a fuel cell (Ivnitski et al., 2006). However, an outstanding challenge for the development of viable biofuel cells is the thermal stability of the functional protein. In this work we have demonstrated a direct correlation between the Cu-$S_{\gamma\text{-Cys}}$ bond and the relation between thermal stability and oxidation state of the enzyme. Moreover, we have shown how this critical bond length can be tuned by amino acid substitutions far from the copper metal

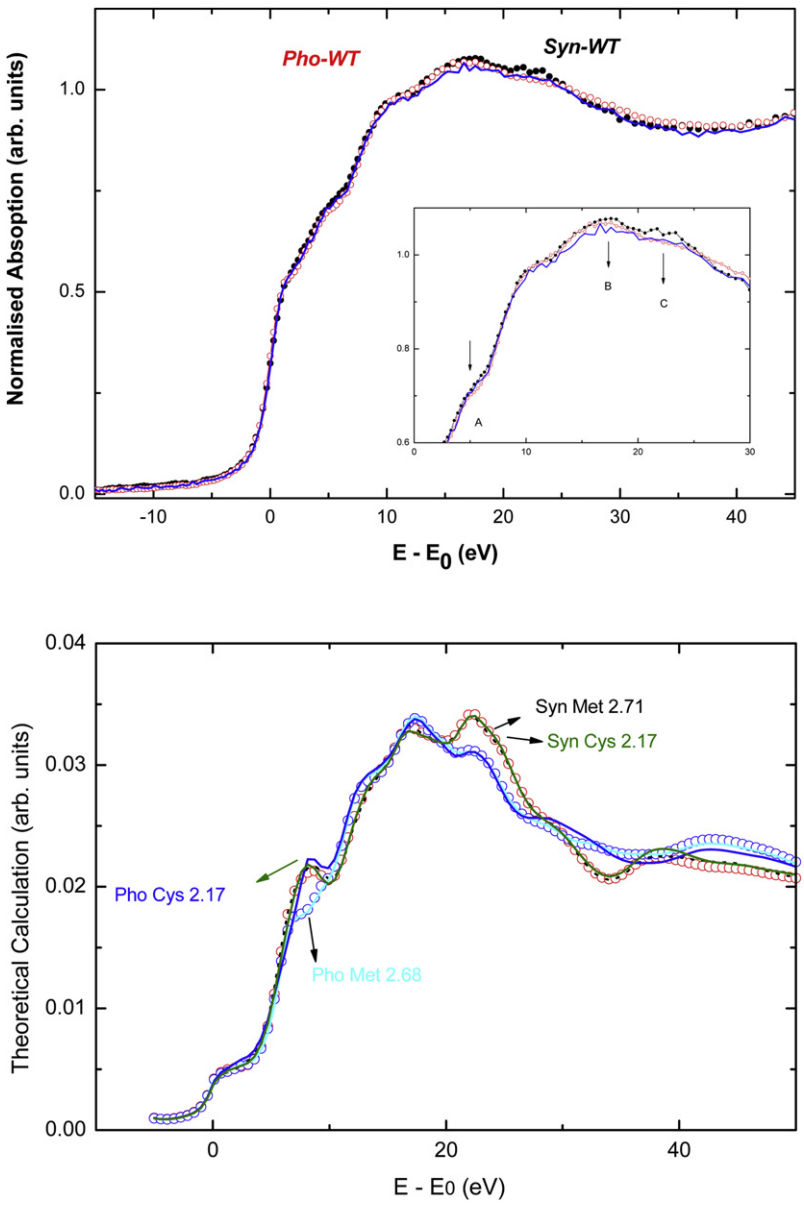

Figure 4. XANES of the Reduced Forms

The top panel shows a detailed comparison of the experimental XANES spectrum at the Cu K-edge of the reduced Pc in *Synechocystis* (●) and *Phormidium* (○). The dotted blue line corresponds to the spectrum recorded in the case of *Pho*-Mut. The bottom panel shows a comparison of the theoretical spectra calculated for *Syn*-WT (○) and *Pho*-WT (○) by adopting the structural Cu environment of the oxidized forms and those in which the Cu-$S_{\gamma,Cys}$ and Cu-$S_{\delta,Met}$ bond lengths are fixed to intermediate values between those found in the oxidized forms.

center. This represents an excellent model of a long-range interplay between the metal site and the protein matrix.

Thus, we believe that the findings presented in this paper are crucial for attempting a rational design of highly thermally stable enzymes with potential biotechnological applications (Marshall et al., 2009; Lancaster et al., 2009).

EXPERIMENTAL PROCEDURES

The computation of the Cu K-edge XANES spectra was carried out using the multiple-scattering code CONTINUUM. A complete discussion of the procedure can be found elsewhere (Chaboy and Quartieri, 1995; Chaboy et al., 2007b), and the details of these computations are reported in the Supplemental Experimental Procedures. Special attention has been given to the choice of the exchange and correlation part of the final state potential (Chaboy et al., 2007a, 2007b; Hatada and Chaboy, 2007) and to the interplay of the $3d^9$ and $3d^{10}\underline{L}$ electronic configurations into reproducing the experimental Cu(II) K-edge XANES spectra (Chaboy et al., 2005, 2006a, 2006b).

The theoretical spectra have been compared to the experimental data reported by Muñoz-López et al. (2010a). For the comparisons the experimental XANES spectra were normalized, after background subtraction, at high energy (~100 eV above the edge) to eliminate thickness dependence. The calculated theoretical spectra have been further convoluted with a Lorentzian shape function (Γ = 1.5 eV) to account for the core-hole lifetime (Krause and Oliver, 1979) and the experimental resolution.

SUPPLEMENTAL INFORMATION

Supplemental Information includes Supplemental Experimental Procedures and two figures and can be found with this article online at doi:10.1016/j.chembiol.2010.12.006.

ACKNOWLEDGMENTS

This work was partially supported by CICYT-MAT2008-06542-C04 and BFU2009-07190 grants of the Spanish Ministry of Science and Innovation, and by the Andalusian Government (BIO-198 and P06-CVI-01713). The authors declare that they have no competing financial interests.

Received: October 6, 2010
Revised: December 9, 2010
Accepted: December 10, 2010
Published: January 27, 2011

REFERENCES

Adams, M.W.W., and Kelly, R.M. (1995). Enzymes from microorganisms in extreme environments. Chem. Eng. News *73*, 32–42.

Alcaraz, L.A., and Donaire, A. (2004). Unfolding process of rusticyanin: evidence of protein aggregation. Eur. J. Biochem. *271*, 4284–4292.

Alcaraz, L.A., and Donaire, A. (2005). Rapid binding of copper(I) to folded aporusticyanin. FEBS Lett. *579*, 5223–5226.

Arcangeli, C., Bizzarri, A.R., and Cannistraro, S. (2001). Molecular dynamics simulation and essential dynamics study of mutated plastocyanin: structural, dynamical and functional effects of a disulfide bridge insertion at the protein surface. Biophys. Chem. *92*, 183–189.

Bond, C.S., Bendall, D.S., Freeman, H.C., Guss, J.M., Howe, C.J., Wagner, M.J., and Wilce, M.C.J. (1999). The structure of plastocyanin from the cyanobacterium *Phormidium laminosum*. Acta Crystallogr. D Biol. Crystallogr. *55*, 414–421.

Canters, G.W., Kolczak, U., Armstrong, F., Jeuken, L.J.C., Camba, R., and Sola, M. (2000). The effect of pH and ligand exchange on the redox properties of blue copper proteins. Faraday Discuss. *116*, 205–220.

Chaboy, J. (2009). Relationship between the structural distortion and the Mn electronic state in La1-xCaxMnO3: a Mn K -edge XANES study. J. Synchrotron Radiat. *16*, 533–544.

Chaboy, J., and Quartieri, S. (1995). X-ray absorption at the Ca K-edge in natural-garnet solid solutions: a full-multiple-scattering investigation. Phys. Rev. B Condens. Matter *52*, 6349–6357.

Chaboy, J., Muñoz-Páez, A., Carrera, F., Merkling, P., and Sánchez-Marcos, E. (2005). *Ab initio* x-ray absorption study of copper *K*-edge XANES spectra in Cu(II) compounds. Phys. Rev. B *71*, 134208.

Chaboy, J., Muñoz-Páez, A., and Sánchez-Marcos, E. (2006a). The interplay of the $3d^9$ and $3d^{10}L$ electronic configurations in the copper K-edge XANES spectra of Cu(II) compounds. J. Synchrotron Radiat. *13*, 471–476.

Chaboy, J., Muñoz-Páez, A., Merkling, P., and Sánchez-Marcos, E. (2006b). The hydration of Cu^{2+}: can the Jahn-Teller effect be detected in liquid solution? J. Chem. Phys. *124*, 64509.

Chaboy, J., Maruyama, H., and Kawamura, N. (2007a). *Ab-initio* x-ray absorption study of Mn K-edge XANES spectra in Mn_3MC (M = Sn, Zn and Ga) compounds. J. Phys. Condens. Matter *19*, 216214.

Chaboy, J., Nakajima, N., and Tezuka, Y. (2007b). *Ab-initio* x-ray absorption near-edge structure study of Ti K-edge in rutile. J. Phys. Condens. Matter *19*, 266206.

Comba, P. (2000). Coordination compounds in the entatic state. Coord. Chem. Rev. *200-202*, 217–245.

Feio, M.J., Navarro, J.A., Teixeira, M.S., Harrison, D., Karlsson, B.G., and De la Rosa, M.A. (2004). A thermal unfolding study of plastocyanin from the thermophilic cyanobacterium *Phormidium laminosum*. Biochemistry *43*, 14784–14791.

Feio, M.J., Navarro, J.A., Díaz-Quintana, A., Navarro, J.A., and De la Rosa, M.A. (2006). Thermal unfolding of plastocyanin from the mesophilic cyanobacterium *Synechocystis* sp PCC 6803and comparison with its thermophilic counterpart from *Phormidium laminosum*. Biochemistry *45*, 4900–4906.

Gough, J., and Chotia, C. (2004). The linked conservation of structure and function in a family of high diversity: The monomeric cupredoxins. Structure *12*, 917–925.

Guckert, J.A., Lowery, M.D., and Solomon, E.I. (1995). Electronic structure of the reduced blue copper active site: contributions to reduction potentials and geometry. J. Am. Chem. Soc. *117*, 2817–2844.

Harrison, M.D., Yanagisawa, S., and Dennison, C. (2005). Investigating the cause of the alkaline transition of phytocyanins. Biochemistry *44*, 3056–3064.

Hatada, H., and Chaboy, J. (2007). *Ab-initio* x-ray absorption study of Mn and Cu K-edge XANES spectra in Cu_2MnM (M = Al, Sn, In) Heusler alloys. Phys. Rev. B Condens. Matter *76*, 104411.

Ivnitski, D., Branch, B., Atanassov, P., and Apblett, C. (2006). Glucose oxidase anode for biofuel cell based on direct electron transfer. Electrochem. Commun. *8*, 1204–1210.

Jones, L.H., Liu, A.M., and Davidson, V.L. (2003). An engineered Cu-A amicyanin capable of intermolecular electron transfer reactions. J. Biol. Chem. *278*, 47269–47274.

Kosman, D.J. (2010). Multicopper oxidases: a workshop on copper coordination chemistry, electron transfer, and metallophysiology. J. Biol. Inorg. Chem. *15*, 15–28.

Krause, M.O., and Oliver, J.H. (1979). Natural widths of atomic K and L levels, K_α X-ray lines and several KLL auger lines. J. Phys. Chem. Ref. Data *8*, 329–338.

LaCroix, L.B., Shadle, S.E., Wang, Y., Averill, B.A., Hedman, B., Hodgson, K.O., and Solomon, E.I. (1996). Electronic structure of the perturbed blue copper site in nitrite reductase: spectroscopic properties, bonding, and implications for the entatic/rack state. J. Am. Chem. Soc. *118*, 7755–7768.

Lancaster, K.M., DeBeer, G.S., Yokohama, K., Richards, J.H., and Gray, H.B. (2009). Type-zero copper proteins. Nat. Chem. *1*, 711–715.

Landau, M., Mayrose, I., Rosenberg, Y., Glaser, F., Martz, E., Pupko, T., and Ben-Tal, N. (2005). ConSurf 2005: the projection of evolutionary conservation scores of residues on protein structures. Nucleic Acids Res. *33*, W299–W302.

Leckner, J., Wittung, P., Bonander, N., Karlsson, B.G., and Malmstrom, B.G. (1997). The effect of redox state on the folding free-energy of azurin. J. Biol. Inorg. Chem. *2*, 368–371.

Lehmann, M., Pasamontes, L., Lassen, S.F., and Wyss, M. (2000). The consensus concept for thermostability engineering of proteins. Biochim. Biophys. Acta *1543*, 408–415.

Marshall, N.M., Garner, D.K., Wilson, T.D., Gao, Y.G., Robinson, H., Nilges, M.J., and Lu, Y. (2009). Rationally tuning the reduction potential of a single cupredoxin beyond the natural range. Nature *462*, 113–116.

Muñoz-López, F.J., Frutos-Beltrán, E., Díaz-Moreno, S., Díaz-Moreno, I., Subías, G., De la Rosa, M.A., and Díaz-Quintana, A. (2010a). Modulation of copper site properties by remote residues determines the stability of plastocyanins. FEBS Lett. *584*, 2346–2350.

Muñoz-López, F.J., Raugei, S., De la Rosa, M.A., Díaz-Quintana, A., and Carloni, P. (2010b). Changes in non-core regions stabilise plastocyanin from the thermophilic cyanobacterium *Phormidium laminosum*. J. Biol. Inorg. Chem. *15*, 329–338.

Miura, Y., Tsujimura, S., Kurose, S., Kamitaka, Y., Kataoka, K., Sakurai, T., and Kano, K. (2009). Direct electrochemistry of CueO and its mutants at residues to and near a type I Cu for oxygen-reducing biocathode. Fuel Cells *9*, 70–78.

Nakamura, K., and Go, N. (2005). Function and molecular evolution of multicopper blue proteins. Cell. Mol. Life Sci. *62*, 2050–2066.

Pavelka, M., and Burda, J.V. (2008). Computational study of redox active centres of blue copper proteins: a computational DFT study. Mol. Phys. *106*, 2733–2748.

Persidis, A. (1998). Extremophiles. Nat. Biotechnol. *16*, 593–594.

Pettersen, E.F., Goddard, T.D., Huang, C.C., Couch, G.S., Greenblatt, D.M., Meng, E.C., and Ferrin, T.E. (2004). UCSF Chimera—a visualization system for exploratory research and analysis. J. Comput. Chem. *25*, 1605–1612.

Pozdnyakova, I., and Wittung-Stafshede, P. (2001). Biological relevance of metal binding before protein folding. J. Am. Chem. Soc. *123*, 10135–10136.

Pozdnyakova, I., Guidry, J., and Wittung-Stafshede, P. (2001). Probing copper ligands in denatured *Pseudomonas aeruginosa* azurin: Unfolding His117Gly and His46Gly mutants. J. Biol. Inorg. Chem. *6*, 182–188.

Randall, D.W., Gamelin, D.R., LaCroix, L.B., and Solomon, E.I. (2000). Electronic structure contributions to electron transfer in blue Cu and Cu(A). J. Biol. Inorg. Chem. *5*, 16–19.

Remenyi, R., Jeuken, L.J.C., Comba, P., and Canters, G.W. (2001). An amicyanin C-terminal loop mutant where the active-site histidine donor cannot be protonated. J. Biol. Inorg. Chem. *6*, 23–26.

Romero, A., De la Cerda, B., Varela, P.F., Navarro, J.A., Hervás, M., and De la Rosa, M.A. (1998). The 2.15 A crystal structure of a triple mutant plastocyanin from the cyanobacterium *Synechocystis* sp. PCC 6803. J. Mol. Biol. *275*, 327–336.

Sandberg, A., Harrison, D.J., and Karlsson, B.G. (2003). Thermal denaturation of spinach plastocyanin: Effect of copper site oxidation state and molecular oxygen. Biochemistry *42*, 10301–10310.

Sato, K., and Dennison, C. (2002). Effect of histidine 6 protonation on the active site structure and electron-transfer capabilities of pseudoazurin from Achromobacter cycloclastes. Biochemistry *41*, 120–130.

Solomon, E.I. (2006). Spectroscopic methods in bioinorganic chemistry: blue to green to red copper sites. Inorg. Chem. *45*, 8012–8025.

Solomon, E.I., Gorelsky, S.I., and Dey, A. (2006). Metal-thiolate bonds in bioinorganic chemistry. J. Comput. Chem. *27*, 1415–1428.

Solomon, E.I., Szilagyi, R.K., George, S.D., and Basumallick, L. (2004). Electronic structures of metal sites in proteins and models: contributions to function in blue copper proteins. Chem. Rev. *104*, 419–458.

Szilagyi, A., and Zavodszky, P. (2000). Structural differences between mesophilic, moderately thermophilic and extremely thermophilic protein subunits: results of a comprehensive survey. Structure *8*, 493–504.

Tsujimura, S., Miura, Y., and Kano, K. (2008). CueO-immobilized porous carbon electrode exhibiting improved performance of electrochemical reduction of dioxygen to water. Electrochim. Acta *53*, 5716–5720.